# Pulsed field ionization-photoelectron photoion coincidence spectroscopy with synchrotron radiation: The heat of formation of the $C_2H_5^+$ ion

**Tomas Baer,*[a] Y. Song,[bc] Jianbo Liu,[b] Wenwu Chen[b] and C. Y. Ng[c]**

[a] *Department of Chemistry, University of North Carolina, Chapel Hill, NC 27599-3290, USA*
[b] *Lawrence Berkeley National Laboratory Chemical Sciences Division, Berkeley, CA 94720, USA*
[c] *Department of Chemistry, Iowa State University, Ames, IA 50011, USA*

***Received 6th December 1999***
***Published on the Web 17th April 2000***

Pulsed field ionization photoelectron (PFI-PE) spectroscopy combined with ion coincidence detection has been used with multi-bunch synchrotron radiation at the Advance Light Source (ALS) to energy select ions and to measure their breakdown diagram. The resolution for ion state selection achieved with $Ar^+$ ($^2P_{3/2,\,1/2}$) employing this PFI-PE-photoion coincidence apparatus is 0.6 meV (full width at half maximum). The production of $C_2H_5^+$ from $C_2H_5Br$ was investigated near the dissociative photoionization limit with this pulsed field ionization-threshold photoelectron photoion coincidence (PFI-PEPICO) scheme. Although the PFI-PE spectra of $C_2H_5Br$, $C_2H_5I$, and benzene show that the production of ions in the Franck–Condon gap regions is quite low, the selectivity for PFI-PE detection and the suppression of prompt electrons is such that we can detect 1 PFI-PE out of 25 000 total electrons $s^{-1}$. The derived $C_2H_5^+$ heat of formation from the analysis of the $C_2H_5Br^+$ breakdown diagram and a critical analysis of other results is 900.5 $\pm$ 2.0 kJ $mol^{-1}$ at 298 K, or 913.2 $\pm$ 2.0 kJ $mol^{-1}$ at 0 K. This leads to an ethylene proton affinity at 298 K of 682.0 kJ $mol^{-1}$. The measured IE of $C_2H_5Br$ is 10.307 eV.

## Introduction

The dissociation dynamics and dissociation onsets for ionic reactions have been investigated during the past thirty years by the technique of threshold photoelectron photoion coincidence (TPEPICO) spectrometry.[1] In this approach, threshold photoelectrons, TPE, (usually with initial energies less than about 20 meV) are collected in delayed coincidence with their corresponding ions. By energy conservation, the coincident ions have an energy equal to $h\nu - \mathrm{IE} + E_{\mathrm{th}}$, where $h\nu$ is the photon energy, IE is the molecule's ionization energy, and $E_{\mathrm{th}}$ is the molecule's thermal internal energy prior to ionization. The success of TPEPICO lies in the high efficiency with which TPE are collected, and energetic electrons are rejected when ions and electrons are extracted by a small dc electric field. However, it has proven difficult to improve the resolution of TPE spectroscopy to better than about 5 meV.[2] In addition, unless the light source is pulsed, as in the case of synchrotron radiation operated in the one or two bunch mode, the analyzer function for TPEs

contains a long tail toward the high energy side as a result of the energetic or "hot" electrons that are photo-ejected in the direction of the electron detector.

The remarkable improvement in electron resolution offered by the pulsed field ionization (PFI) approach to the detection of zero kinetic energy electrons[3,4] has permitted the determination of IEs and vibrational frequencies with sub-wavenumber accuracy (<0.1 meV). In this approach, long lived atomic or molecular species in high-*n* Rydberg states ($n > 100$) are formed by photoexcitation and stored in very low electric fields for up to several microseconds during which time any background prompt electrons are removed from the ionization region. Upon the application of a small pulsed electric field, the Rydberg states are field ionized and the PFI-PE detected with little interference from the prompt background electrons. Thus the difference between TPE and PFI-PE spectroscopy is that in the former, the detected electrons are formed slightly above the IE, while in the latter, the detected electrons are formed slightly below the IE.

Although the resolution is excellent, laser based PFI-PE detection is not well suited for PEPICO studies because in the usual 10–30 Hz pulsed laser sources used to generate the high Rydberg states many ions are formed at the same time. Thus, it is not possible to collect ions in coincidence with PFI-PEs. The repetition rate of the ionization laser would have to be greater than about 1 kHz in order to keep the total ion production rate to less than 10% per laser shot. However, as shown by Zhu and Johnson some years ago,[5] it is possible to prepare ions in selected energy states by the mass analyzed threshold ionization (MATI) approach in which the ions produced by field ionization are distinguished from the directly generated or prompt ions using a separating electric field. The problem with this method is that relatively high electric fields are required to separate the direct ions from the Rydberg states thereby depleting the population of high-*n* Rydberg states and thus limiting the MATI signal to those Rydberg states with intermediate *n* values. Consequently, the signal is significantly lower than that in a typical PFI-PE experiment. The main advantage of MATI is that ions are mass as well as energy selected. It is thus equivalent to TPEPICO detection, but with an energy resolution that is two orders of magnitude higher.

We present here the PFI-PEPICO scheme, which can be viewed as an alternative to MATI. In this method, the light source is dispersed synchrotron radiation that operates in the multi-bunch mode. The method is illustrated for the dissociation of $C_2H_5Br^+$. In addition, we present some PFI-PE spectra and their corresponding photoionization efficiency (PIE) curves for Ar, $C_2H_5Br$, $C_2H_5I$, and benzene. Of interest is the intensity of PFI signal in the Franck–Condon gaps between the ion's electronic states. In TPE spectroscopy, these Franck–Condon gaps are generally filled with electron signal. The mechanism for the formation ion signal in the Franck–Condon gaps has been shown to be related to the dissociation to neutral products,[6] and a mechanism for their formation has been proposed.[6,7] Because the observation of fragment ion signal at the dissociation thresholds that often fall in these Franck–Condon gap regions depends on the production of TPEs, it is of interest to determine whether PFI-PEs will also be produced in these Franck–Condon gap regions.

## Experimental approach

The experimental arrangement and procedures for PFI-PE[8,9] and the recent extension to PFI-PEPICO measurements have been thoroughly discussed.[10,11] Synchrotron radiation from an undulator is dispersed by a 6.5 m Eagle-mounted monochromator. The ring, operated in the multi-bunch mode, generates 512 ns of quasi-continuous radiation followed by a 144 ns dark gap. The photons excite the molecular beam cooled sample in the presence of a 0.2 V $cm^{-1}$ dc electric field to energies in the vicinity of the dissociative ionization threshold. While the promptly produced electrons are extracted by the small dc field, neutrals in high-*n* Rydberg states remain in the ion source. They are stabilized by the low dc, or stray electric fields through Stark mixing of the P and $m_p$ states.[12] These high-*n* and high-P Rydberg states are then field ionized during the 144 ns dark gap by a 7.3 V $cm^{-1}$, 200 ns long pulsed electric field. The PFI-PEs are collected in a 5 ns time window that serves to discriminate against all non-field-ionized electrons produced by direct ionization. The success of this experiment is due to the very high photon resolution (<0.001 eV) of the 6.5 m monochromator[13] that permits excitation of a narrow band of high-*n* Rydberg states

and the 144 ns dark period of the synchrotron that permits their field ionization in the absence of prompt electrons.

Ions are extracted by the constant dc field of 0.2 V $cm^{-1}$ as well as by the 1.52 MHz, 7.3 V $cm^{-1}$ pulsed field. The $C_2H_5Br^+$ parent ions spend about 7 μs in the pulsed 6 mm acceleration region, while the product $C_2H_5^+$ daughter ions spend 3.5 μs there. Thus, they require on the average 10.5 and 5 pulsing cycles to exit this first acceleration region. The average electric field in this quasi-continuous acceleration region is about 3 V $cm^{-1}$. Typical collection efficiencies for Ar at its IE were 6% for PFI-PEs and 30% for ions.

The PFI-PEs and ions provided the start and stop signals respectively for a Stanford Research Systems multi-channel scalar. The ion TOF resolution used in this study was 40 ns per channel. Time-of-flight (TOF) spectra were collected at fixed photon energies. The PFI signal for $C_2H_5Br$ was not high because the interesting dissociation region is located in the Franck–Condon gaps between the ground and the A state. In addition, the high energy resolution necessarily reduces the number of electrons within the narrow energy window. Typical count rates were 1 count $s^{-1}$ PFI-PEs, 23 000 counts $s^{-1}$ ions, and 0.2 count $s^{-1}$ coincidence events. Most ion TOF distributions were collected over a period of 1–2 h. All ions were collected with no suppression of "false" ions. It was necessary in many cases to close the slits in order to keep the total ion count rates down to avoid the build up of a false coincidence background. Some planned modifications may improve the signal to noise ratio in future experiments. One is the installation of a fast ion gate which will permit only ions associated with a PFI electron to be collected thereby dramatically reducing the false coincidence counts. A second change is the replacement of the current low voltage pulser with a 100 V pulser generator. The applied pulse would be applied in two steps. First a small 4 V $cm^{-1}$ pulse of 20 ns duration to extract the PFI electrons followed by the 100 V pulse to extract the ions. This will reduce the width of the ion TOF peaks and thus improve the signal to noise ratio. Finally, it may be possible to install a time varying field[14] that may help stabilize the high-*n* Rydberg states thereby increasing the yield of PFI-PEs.

The vapor of the $C_2H_5Br$, $C_2H_5I$, and $C_6H_6$ samples were diluted in Ar in a seed ratio of about 30% and expanded through a 90 μm nozzle. Argon was chosen in part because it provides for cooling without giving the sample too high a velocity perpendicular to the ion extraction field. Upon ionization, the ions were accelerated to a final energy of 120 eV through three acceleration regions, and travelled with this energy through the 40 cm long drift tube where they were ultimately detected by a set of microchannel plates. The translational temperature of the molecular beam as measured from the TOF peak widths was about 30 K. However, this is not necessarily a good measure of the internal energy of the molecules in the beam.[15,16]

## Results

### PFI and PIE spectra

Figs. 1 to 4 show the PFI-PE spectra along with the photoionization efficiency (PIE) curves for Ar, $C_2H_5Br$, $C_2H_5I$, and benzene. These spectra were collected under identical conditions so that the intensities can be compared to each other. The scale on the left ordinate refers to the PIE signal while the scale on the right refers to the PFI-PEs. Note that the Ar spectral intensities are about two orders of magnitude greater than those for the molecules. The Ar PIE spectrum shows the usual s and d Rydberg series that converge to the higher spin–orbit state of the $Ar^+$ ($^2P_{1/2}$). The PFI-PE spectrum shows just the two peaks that correspond to the two electronic states. The resolution, limited primarily by the photon resolution, is 1 meV.

The energy scale for the PFI-PE spectra for the other three molecules was calibrated by running scans of Ar and Xe. The width of the origin band for $C_2H_5Br$ is 4.5 meV, which is most probably determined by the rotational temperature of the $C_2H_5Br$ in the molecular beam. The intensity of the PFI peak relative to the total ion peak is considerably less in the case of $C_2H_5Br$ than in Ar. In the case of Ar, the peaks were about equal whereas in $C_2H_5Br$, the PFI peak is weaker by a factor of 20. The $C_2H_5Br$ IE is 10.307 eV and the higher spin–orbit state lies at 10.614 eV. No other PFI-PE spectra have been published for this molecule.

The PFI-PE spectrum of $C_2H_5I$ is similar to that of $C_2H_5Br$ except that the spin–orbit splitting is larger and the intensity of the PFI-PE peak relative to the ion peak is now 1 : 5, rather than

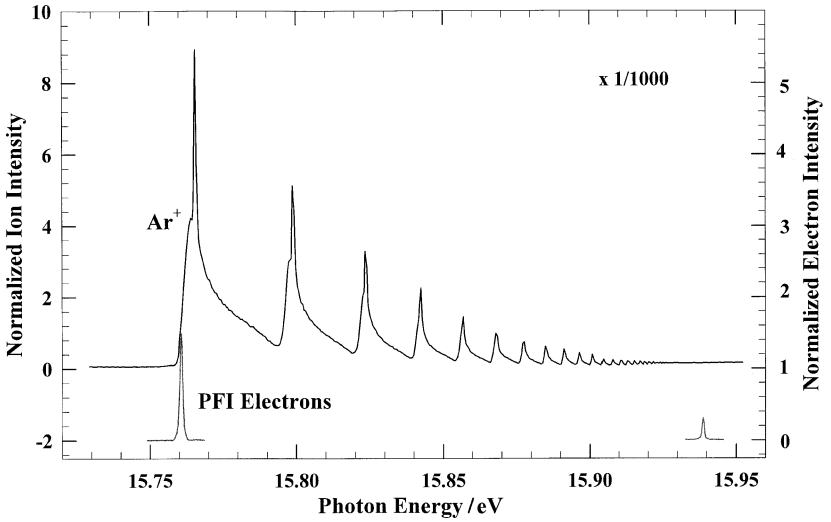


**Fig. 1** The photoionization efficiency (PIE) spectrum of total Ar ions as a function of photon energy and the pulsed field ionization photoelectron (PFI-PE) spectrum in the vicinity of the $^2P_{3/2}$ ground state and the $^2P_{1/2}$ excited spin–orbit state of $Ar^+$. The signal intensities should be multiplied by a factor of 1000 before comparing to the signal levels in the other spectra.

1 : 20. The peak width of the origin peak is 5.4 meV. In addition it shows a strong asymmetry toward lower energies which is characteristic of PFI-PE peaks in which the resolution is determined by the intensity of the extraction pulse (3.5 V $cm^{-1}$). The $C_2H_5I$ IE and the upper spin–orbit state is 9.351 and 9.935 eV, which compares well with a previous PFI-PE study in which

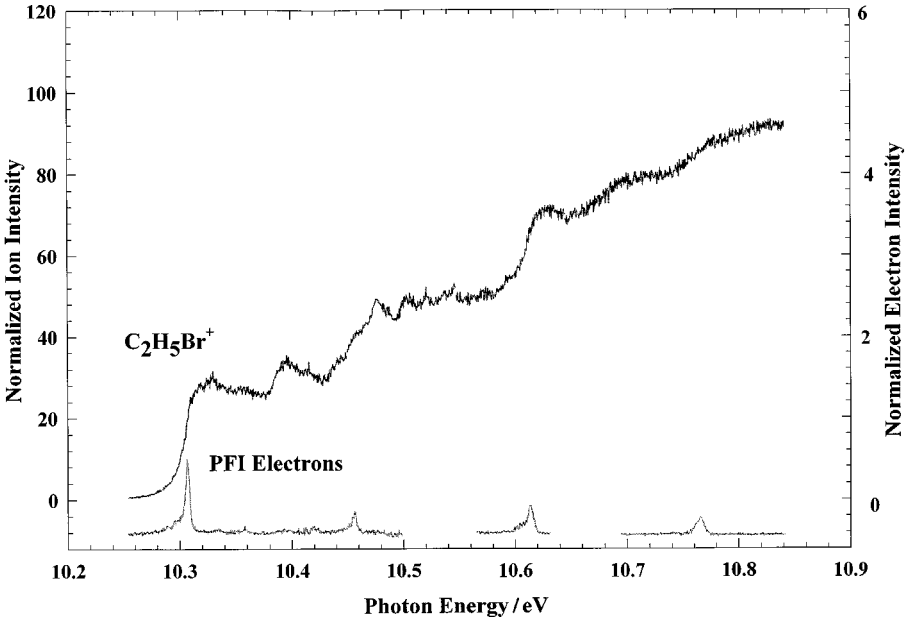


**Fig. 2** The photoionization efficiency (PIE) spectrum of total $C_2H_5Br^+$ ions as a function of the photon energy and the PFI-PE spectrum of $C_2H_5Br$. The PFI-PE peak at 10.45 eV is due to a vibration in the ground spin–orbit state of the ion. The peak at 10.6 eV is the second spin–orbit state of $C_2H_5Br^+$, while the final peak at 10.76 eV is a vibration associated with the upper spin–orbit state of $C_2H_5Br^+$.

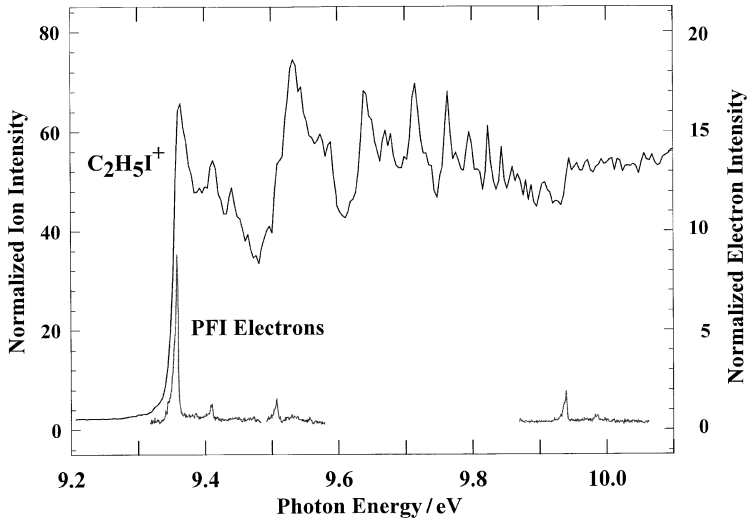


**Fig. 3** The photoionization efficiency (PIE) spectrum of total $C_2H_5I^+$ ions as a function of the photon energy and the PFI-PE spectrum of $C_2H_5I$. The PFI peaks at 9.4 and 9.5 eV are vibrations associated with the ground electronic state, while the peak at 9.93 eV is the origin of the upper spin–orbit state of $C_2H_5I^+$.

Knoblauch *et al.*[17] reported energies of 9.349 and 9.932 eV, respectively. The Rydberg series shown in the PIE spectrum are considerably more pronounced in $C_2H_5I$ than they are in the $C_2H_5Br$.

The final spectrum is that of benzene which is shown mainly to illustrate the method for a larger polyatomic and because benzene is a standard PFI-PE molecule. Here the PFI-PE peak intensity relative to that for the ion peak is about 1 : 5. The measured benzene ionization energy

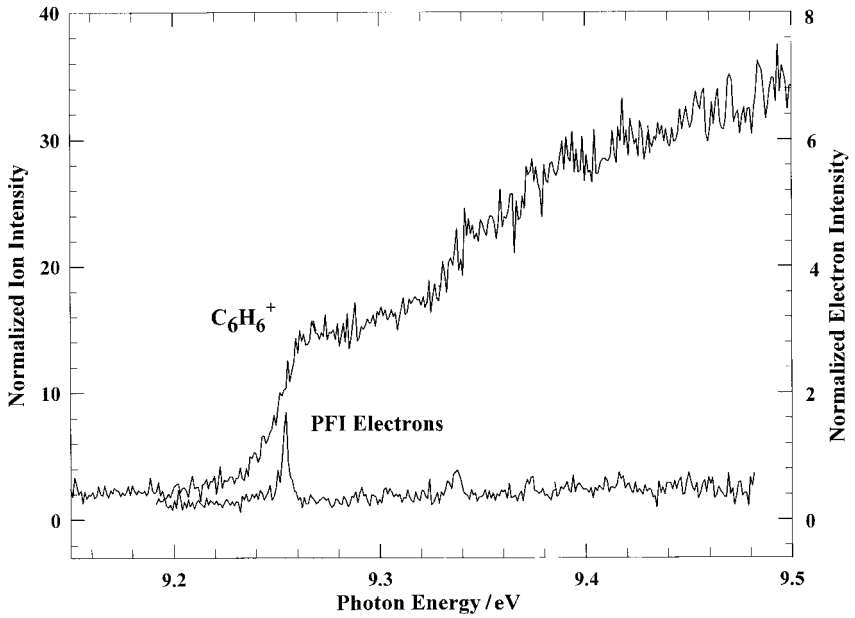


**Fig. 4** The photoionization efficiency (PIE) spectrum of total $C_6H_6^+$ ions as a function of the photon energy and the PFI-PE spectrum of $C_6H_6$. The very weak PFI peak at 9.34 eV seems to be associated with a large increase in the PIE signal.

of 9.245 eV is close to 9.2438 eV as recently reported by Neuhauser *et al.*[18] Of particular interest is the step in the PIE spectrum at around 9.34 eV. This strong step is associated with the excitation of two vibrational states that are about half of the intensity of the transition origin in the threshold photoelectron spectrum.[19] In contrast, the two PFI-PE peaks at 9.34 and 9.375 eV are extremely weak. Apparently, the high Rydberg states that are produced in this region decay by other channels and thus do not yield much PFI-PE signal.

These spectra are shown to illustrate the relative intensities of PFI-PE and ion signals. It is evident that this ratio is very favorable for the case of Ar, and less so for the molecules. In the case of $C_2H_5Br$, the ratio is very low. Apparently the high-$n$ Rydberg states in these molecules are less stable than the high-$n$ states in Ar so that they decay to ions more efficiently in the small applied field of 0.2 V $cm^{-1}$. This reduced efficiency of PFI-PE production in molecules is of considerable importance in the PFI-PEPICO experiment because it reduces the ratio of real to false coincidence signal.

The other aspect of the PFI-PE spectra that is of importance to the PFI-PEPICO experiment is the PFI-PE signal in Franck–Condon gaps. Whereas TPE spectra have significant signal at essentially all photon energies,[6,20–23] the PFI-PE signal nearly vanishes in between the Franck–Condon allowed regions of the spectrum. This means that energy selection of ions with PFI-PEPICO may be more restricted than it is in TPEPICO.

### $C_2H_5Br$ PFI-PEPICO data

Fig. 5 shows representative PFI-PEPICO TOF data for the $C_2H_5Br$ molecule at several photon energies below and above the dissociation limit for the loss of Br. In these experiments, the total ion signal was about 23 000 counts $s^{-1}$, while the PFI-PE signal was about 1 count $s^{-1}$. The data indicate that nearly all of the PFI-PE signal collected was due to true PFI-PEs. That is, our experiment successfully suppressed 23 000 prompt electrons per second. The statistics of PEPICO experiments permits the calculation of electron and ion collection efficiencies as well as the number of false coincidences per time interval, $\Delta T$, by the following relationships:[24,25] PFI-PE detection efficiency = $C/I$; ion detection efficiency = $C$/PFIE; and false coincidences = (counts from electron detector)($I$)($\Delta T$) in which $C$ is the coincidence rate in counts $s^{-1}$, $I$ is the total ion count rate in counts $s^{-1}$, and PFIE is the PFI-PE rate in counts $s^{-1}$. The false coincidence rate is determined by the total counts at the electron detector, including any background counts which may become significant when the true PFI-PE rate is low. The ion detection efficiencies measured in these studies varied between 10 and 30% depending on the experimental conditions. For the

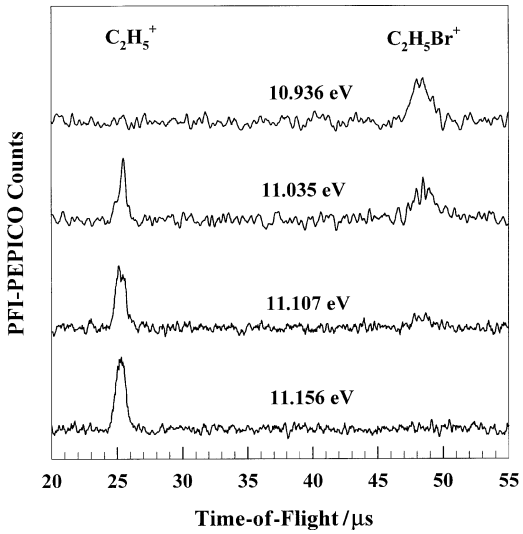


**Fig. 5** Some representative ion time of flight distributions of $C_2H_5^+$ and $C_2H_5Br^+$ ions in the vicinity of the dissociation limit.

case of the $C_2H_5Br$ data at 10.936 eV in Fig. 5, the value was 10%. Thus the false coincidences collected in a 3.2 μs time interval is given by (1 count $s^{-1}$)(24 800 counts $s^{-1}$)(3.2 μs) = 0.080 counts $s^{-1}$, while the number of real coincidences was electron counts times the ion efficiency, or (1 count $s^{-1}$)(0.10) = 0.10. Thus the ratio of real to false signal is 0.10/0.08 = 1.25, while the measured value from Fig. 5 is 1.30.

### Ethyl bromide ion breakdown diagram and the $\Delta_f H°(C_2H_5^+)$

The breakdown diagram for $C_2H_5Br^+$ is shown in Fig. 6. This is a plot of the fractional amount of $C_2H_5^+$ and $C_2H_5Br^+$ as a function of the photon energy (*hν*). If the ions were produced from molecules at 0 K (with no internal energy) and the energy resolution were infinitely good, the breakdown diagram should be given by two step functions in which the parent ion signal goes from 1 to 0 and the daughter ion signal goes from 0 to 1 at the dissociation limit. Because of the thermal energy of the ions and also because of an apparent increase of the PFI-PE yield with thermal energy content,[16] the breakdown diagram deviates from the ideal. We can model the breakdown diagram by calculating the thermal energy distribution $P(E, T)$ at some temperature and thereby obtain the daughter and parent ion signal by eqns. (1) and (2).

$$\text{Daughter}(h\nu) = \int_{\text{AE}-h\nu \text{ or } 0}^{\infty} P(E, T)\, dE \tag{1}$$

$$\text{Parent}(h\nu) = \int_{0}^{\text{AE}-h\nu \text{ or } 0} P(E, T)\, dE \tag{2}$$

The parent ion integral is valid only up to a photon energy that is equal to the 0 K appearance energy (AE). Beyond that energy, all parent ion signal disappears. This 0 K appearance energy of 11.130 ± 0.005 eV is shown by an arrow in Fig. 6.

The only other value for the Br loss onset from the ethyl bromide ion was obtained by Traeger and McLoughlin[26] who reported a 298 K AE of 11.06 ± 0.01 eV on the basis of a photoionization study. This value can be converted to 11.12 eV at 0 K by the addition of the average thermal internal energy of $C_2H_5Br$.

In order to determine the heat of formation of the $C_2H_5^+$ ion, the ethyl bromide heat of formation must be known. As shown in Table 1, the $\Delta_f H°_{298\,K}(C_2H_5Br)$ is listed as −64.52 kJ $mol^{-1}$ by Wagman *et al.*[27] with no error bars and no source attribution, and as −61.9 ± 1.7 kJ $mol^{-1}$ by the later compilation of Pedley *et al.*[28] According to the NIST Webbook[29] the original experimental values range from −61.9 to −65.3 kJ $mol^{-1}$ with an average error of ±2 kJ $mol^{-1}$.

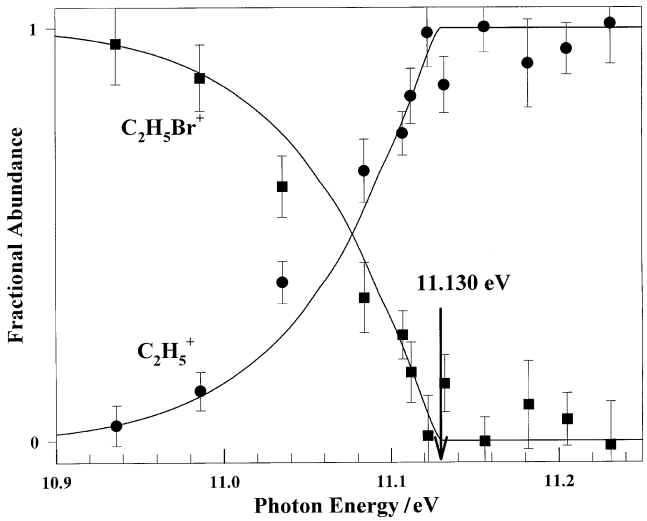


**Fig. 6** The ethyl bromide ion breakdown diagram. The arrow points to the 0 K dissociation limit at 11.130 ± 0.005 eV.

**Table 1** The thermochemistry of the $C_2H_5Br/C_2H_5Br^+$ system

| Molecule | $\Delta_f H^\circ_{298\,K}$ /kJ mol$^{-1}$ | $\Delta_f H^\circ_{0\,K}$ /kJ mol$^{-1}$ | IE /eV | $AE_{0\,K}(C_2H_5{}^+)$ /eV |
|---|---|---|---|---|
| $C_2H_5Br$ | $-64.52^a$ | $-42.63^a$ | $10.307 \pm 0.002^b$ | $11.13 \pm 0.005^b$ |
| | $-61.9 \pm 1.7^c$ | $-39.8 \pm 1.7^d$ | | $11.135 \pm 0.010^e$ |
| Br | $111.9^f$ | $117.9^f$ | | |
| $C_2H_5{}^+$ | $900.6^g$ | $913.2 \pm 2^h$ | | |
| | 903.5 | $916.2 \pm 2^i$ | | |
| | $904.0 \pm 2$ | $916.6 \pm 2^j$ | | |
| | $900.2 \pm 2^k$ | $912.8 \pm 2^k$ | | |

*a* Wagman *et al.* (ref. 27). *b* This work. *c* Pedley *et al.* (ref. 35). *d* Converted from the 298 K value using vibrational frequencies from Shimanouchi (ref. 36). The resulting $H^\circ_{298\,K} - H^\circ_{0\,K} = 13.45$ kJ mol$^{-1}$. *e* The $C_2H_5Br$ internal energy of 0.075 eV was added to the 298 K AE of Traeger *et al.* (refs. 26 and 37). *f* Cox *et al.* (ref. 38). *g* This work. Converted from the 0 K value using calculated vibrational frequencies from Ruscic *et al.* (ref. 30). The Rosenstock convention is used for the ion heat of formation in which the electron is treated as a particle at 0 K. *h* This work. Derived using the Wagman *et al.* (ref. 27) $C_2H_5Br$ heat of formation. *i* This work. Derived using the Pedley *et al.* (ref. 28) $C_2H_5Br$ heat of formation. *j* Traeger and Kompe value (ref. 37). *k* Determined from the adiabatic IE of the $C_2H_5$ radical (8.117 eV) by Ruscic *et al.* (ref. 30) and their quoted 0 K heat of formation of the radical (129.7 kJ mol$^{-1}$).

Our own theoretical *ab initio* MO effort at the MP2/6-311G** level was directed at obtaining the $\Delta_f H^\circ_{0\,K}(C_2H_5Br)$ *via* the isodesmic reaction: $C_2H_5Br + CH_4 \rightarrow C_2H_6 + CH_3Br$. This assumes experimental values for the heats of formation of $CH_4$, $C_2H_6$, and $CH_3Br$, none of which seems controversial.[27,28] These calculations yielded a value of $-64.3$ kJ mol$^{-1}$ for $\Delta_f H^\circ_{0\,K}(C_2H_5Br)$, thereby supporting the lower Wagman value. Still, the issue is not resolved because the error in the *ab initio* calculation is certainly no less than 4 kJ mol$^{-1}$. All we can really say is that the $\Delta_f H^\circ_{298\,K}(C_2H_5Br)$ lies somewhere between $-62$ and $-64.5$ kJ mol$^{-1}$, a range of 2.6 kJ mol$^{-1}$. It seems that this value in the end determines the error limits for the derived $\Delta_f H^\circ(C_2H_5{}^+)$.

Table 1 summarizes the literature and derived $\Delta_f H^\circ_{298\,K}$ and $\Delta_f H^\circ_{298\,K}$ values for $C_2H_5Br$, Br, and $C_2H_5{}^+$. The last entry for the $\Delta_f H^\circ_{298\,K}(C_2H_5{}^+)$ is based on the IE of the $C_2H_5{}^\cdot$ radical which was measured by Ruscic *et al.*[30] to be $8.117 \pm 0.008$ eV. When this is combined with the heat of formation of the ethyl radical, we can determine a heat of the ethyl ion. The latest experimental value for $\Delta_f H^\circ_{298\,K}(C_2H_5{}^\cdot)$ reported by Brouard *et al.*[31a] is $118.6 \pm 1.7$ kJ mol$^{-1}$ which corresponds to a 0 K value of 129.7 kJ mol$^{-1}$. Very recent calculated results by Marshall[31b] assert these values to be $120.5 \pm 2$ and 131.5 kJ mol$^{-1}$, respectively. These agree within the quoted error with the experimental values. When we add these values to the measured ionization energy of Ruscic *et al.*[30] we obtain a $\Delta_f H^\circ_{0\,K}(C_2H_5{}^+)$ of 912.8 or 914.6 kJ mol$^{-1}$ depending on whether we use the experimental or theoretical value for the free radical heat of formation. Our experimental value based on the dissociative photoionization of $C_2H_5Br$ falls just in between these two values, thereby supporting the Wagman value for the $C_2H_5Br$ heat of formation.

The $\Delta_f H^\circ(C_2H_5{}^\cdot)$ can be used to derive a proton affinity for $C_2H_4$ *via* the reaction: $C_2H_4 + H^+ \rightarrow C_2H_5{}^+$. Assuming a $\Delta_f H^\circ_{298\,K}(C_2H_4)$ 298 K of 52.5 kJ mol$^{-1}$ [28] and a $\Delta_f H^\circ_{298\,K}(H^+)$ of 1530 kJ mol$^{-1}$ [32] (stationary electron convention), we obtain an ethylene proton affinity that ranges from 681.9 to 678.5 kJ mol$^{-1}$, with the higher value more consistent with the Wagman value for $\Delta_f H^\circ_{298\,K}(C_2H_5Br)$. This can be compared to the "accepted" value of 680.5 kJ mol$^{-1}$ [33] and a calculated value of 681.9 kJ mol$^{-1}$.[34] When all of these results are taken together, it would appear that the lower Wagman value for the $C_2H_5Br$ heat of formation is preferred and that the $\Delta_f H^\circ_{298\,K}(C_2H_5{}^+)$ is $900.5 \pm 2.0$ kJ mol$^{-1}$.

## Acknowledgements

This work was supported by the Chemical Sciences Division of the US Department of Energy contracts DE-AC03-76SF00098 and DE-FG02-97ER14776. We also thank Balint Sztaray and Judit Vaik for carrying out the *ab initio* MO calculations of the $C_2H_5Br$ energy.

## References


1 T. Baer, *Adv. Chem. Phys.*, 1986, **64**, 111.
2 F. Merkt, P. M. Guyon and J. W. Hepburn, *Chem. Phys.*, 1993, **173**, 479.
3 K. Muller-Dethlefs and E. W. Schlag, *Annu. Rev. Phys. Chem.*, 1991, **42**, 109.
4 H. Sekiya, R. Lindner and K. Muller-Dethlefs, *Chem. Lett.*, 1993, 485.
5 L. Zhu and P. Johnson, *J. Chem. Phys.*, 1991, **94**, 5769.
6 P. M. Guyon, T. Baer and I. Nenner, *J. Chem. Phys.*, 1983, **78**, 3665.
7 T. Baer, *Annu. Rev. Phys. Chem.*, 1989, **40**, 637.
8 C. W. Hsu, M. Evans, C. Y. Ng and P. Heimann, *Rev. Sci. Instrum.*, 1997, **68**, 1694.
9 G. K. Jarvis, Y. Song and C. Y. Ng, *Rev. Sci. Instrum.*, 1999, **70**, 2615.
10 T. Baer, Y. Song, C. Y. Ng, J. Liu and W. Chen, *J. Phys. Chem. A*, 2000, **104**, 1959.
11 G. K. Jarvis, K. M. Weitzel, M. Malow, T. Baer, Y. Song and C. Y. Ng, *Rev. Sci. Instrum.*, 1999, **70**, 3892.
12 W. A. Chupka, *J. Chem. Phys.*, 1993, **98**, 4520.
13 P. Heimann, K. Koike, C.-W. Hsu, M. Evans, K. T. Lu, C. Y. Ng, A. G. Suits and Y. T. Lee, *Rev. Sci. Instrum.*, 1997, **68**, 1945.
14 R. R. Jones, P. Fu and T. F. Gallagher, *J. Chem. Phys.*, 1997, **106**, 3578.
15 P. M. Mayer and T. Baer, *Int. J. Mass Spectrom. Ion Processes*, 1996, **156**, 133.
16 K. M. Weitzel, M. Malow, G. K. Jarvis, T. Baer, Y. Song and C. Y. Ng, *J. Chem. Phys.*, 1999, **11**, 8267.
17 N. Knoblauch, A. Strobel, I. Fischer and V. E. Bondybey, *J. Chem. Phys.*, 1995, **103**, 5417.
18 R. G. Neuhauser, K. Siglow and H. J. Neuser, *J. Chem. Phys.*, 1997, **106**, 896.
19 W. B. Peatman, T. B. Borne and E. W. Schlag, *Chem. Phys. Lett.*, 1969, **3**, 492.
20 T. Baer, P. M. Guyon, I. Nenner, A. Tabche-Fouhaille, R. Botter, L. F. A. Ferreira and T. R. Govers, *J. Chem. Phys.*, 1979, **70**, 1585.
21 A. C. Parr, A. J. Jason and R. Stockbauer, *Int. J. Mass Spectrom. Ion Processes*, 1978, **26**, 23.
22 A. C. Parr, A. J. Jason, R. Stockbauer and K. E. McCulloh, *Int. J. Mass Spectrom. Ion Processes*, 1979, **30**, 319.
23 H. M. Rosenstock, R. Buff, M. A. A. Ferreira, S. G. Lias, A. C. Parr, R. Stockbauer and J. L. Holmes, *J. Am. Chem. Soc.*, 1982, **104**, 2337.
24 J. H. D. Eland, *Int. J. Mass Spectrom. Ion Processes*, 1972, **8**, 143.
25 T. Baer, in *Gas phase ion chemistry*, ed. M. T. Bowers, Academic Press, New York, 1979, pp. 153–196.
26 J. C. Traeger and R. G. McLoughlin, *J. Am. Chem. Soc.*, 1981, **103**, 3647.
27 D. D. Wagman, W. H. E. Evans, V. B. Parker, R. H. Schum, I. Halow, S. M. Mailey, K. L. Churney and R. L. Nuttall, *The NBS Tables of Chemical Thermodynamic Properties*, *J. Phys. Chem. Ref. Data Vol. 11*, *Suppl. 2:* NSRDS: US Government Printing Office; Washington, 1982.
28 J. B. Pedley, R. D. Naylor and S. P. Kirby, *Thermochemical Data of Organic Compounds*, Chapman and Hall, London, 1986.
29 E. P. Hunter and S. G. Lias, *Proton Affinity Evaluations in NIST Chemistry WebBook; NIST Standard Reference Databas 69*; National Institute of Standards and Technology, http://webbook.nist.gov; Gaithersburg, MD 20899, 1998.
30 B. Ruscic, J. Berkowitz, L. A. Curtiss and J. A. Pople, *J. Chem. Phys.*, 1989, **91**, 114.
31 (*a*) M. Brouard, P. D. Lightfoot and M. J. Pilling, *J. Phys. Chem.*, 1986, **90**, 445; (*b*) P. Marshall, *J. Phys. Chem. A*, 1999, **103**, 4560.
32 S. G. Lias, J. E. Bartmess, J. F. Liebman, J. L. Holmes, R. D. Levin and W. G. Mallard, *Gas Phase Ion and Neutral Thermochemistry*, *J. Phys. Chem. Ref. Data Vol 17*, *Suppl. 1*, NSRDS: US Government Printing Office, Washington, 1988.
33 E. P. L. Hunter and S. G. Lias, *J. Phys. Chem. Ref. Data*, 1998, **27**, 413.
34 B. J. Smith and L. Radom, *J. Am. Chem. Soc.*, 1993, **115**, 4885.
35 J. B. Pedley, R. D. Naylor and S. P. Kirby, *Thermochemical Data of Organic Compounds*, Chapman and Hall, London, 1986.
36 T. Shimanouchi, *Tables of Molecular Vibrational Frequencies*, *Natl. Stand. Ref. Data. Ser.* (*US*, *Nat. Bur. Stand.*) *#39*, US Government Printing Office, Washington, 1972.
37 J. C. Traeger and B. M. Kompe, in *Energetics of Organic Free Radicals*, ed. J. A. Martinno Simoes, A. Greenberg and J. F. Liebman, Chapman & Hall, London, 1996, pp. 59–109.
38 J. D. Cox, D. D. Wagman and V. A. Medvedev, *CODATA Key Values for Thermodynamics*, Hemisphere Publ Corp., New York, 1989.